IOP Conf. Series: Materials Science and Engineering **278** (2017) 012024 doi:10.1088/1757-899X/278/1/012024

The effect of condensation area and operating temperature on heat transfer capacity of a closed loop thermosyphon cooling system for HTS machinery

K Yamaguchi[1], M Miki[1], M Izumi[1], Y Murase[2], T Oryu[2], T Yanamoto[2]

[1] Tokyo University of Marine Science and Technology, 2-1-6, Echu-jima, Koto-ku, Tokyo 135-8533, Japan
[2] Kawasaki Heavy Industries. Ltd, 1-1, Kawasaki-cho, Akashi, Hyogo,673-8666, Japan

E-mail: y.kouta0215@gmail.com

Abstract. A sophisticated cooling system is necessary for applications of high-temperature superconductor (HTS) for electric devices. Among them, status of rotating machine requests to maintain the temperature of HTS field poles under 40 K. We have employed a thermosyphon (TS) as cooling system for HTS rotating machines. The TS cooling is based on natural convection of coolant and does not require a forced circulation. Advantages of the TS cooling system are simple, light weight mechanical composition and high heat transfer coefficient with latent heat. The operating temperature of the TS cooling system depends on the saturation temperature and the pressure of coolant. Thus, the saturation pressure of the TS affects the performance of the TS cooling system. In this paper, we investigate the relationship between the saturation pressure and the condenser heat transfer area. We studied a heat transfer capacity under the heat load with different neon quantities using the TS cooling system. The saturation pressure increases with the heat load and/or condenser temperature increment. Reducing the number of condensers i.e. decrease of condensation area, the saturation pressure increases and the heat transfer capacity decreases. This result shows that the saturation pressure is proportional to the temperature difference between condenser temperature and the saturation temperature calculated by saturation pressure.

1. Introduction

High temperature superconductor (HTS) rotating machine requires light weight, compact and effective cooling systems. It is necessary to control the operating temperature of HTS coils which enable us to optimal control of the machine performance. The cooling power should cancel heat invasion from the torque tube and radiation, in addition to hear generation from the field pole windings. There are two kinds of cooling systems proposed for HTS rotating machines. One is the forced circulation of gaseous helium system to keep HTS coils at 25-40 K [1]. This cooling method was used for prototype ship propulsion motors [2-4]. The other type is natural convection cooling system using a closed loop thermosyphon (TS) technology [2]. The cryomechanical design of this TS system is simple because it is composed of a cryocooler, condenser, adiabatic tubes and evaporator. The design of TS cooling system for HTS motor presents several unique design challenges [5-11].

In many studies, the evaporator is placed inside the rotor and thermally connected to HTS field poles on the rotor while the condenser is stationary and located outside the rotor. Moreover, a horizontal adiabatic tube, running along the rotor centre, is used to convey the coolant between the condenser and evaporator. In this set-up, a cryogenic rotary joint is required to enable relative movement between the static condenser and the rotating evaporator. Our laboratory has been conducting studies of TS cooling systems for 100 kW to megawatt-class HTS machines since 2006 [5-9]. For safe and reliable application, commercially available 1G/2G wires for rotor HTS coil must be cooled to temperatures under 40 K. Neon or neon-helium mixture as cryogen provides a suitable operating temperature range of 28-40 K for HTS field pole magnets [5-6]. HTS motors are being considered for application in ship-propulsion. The performance of TS cooling system at sea has been studied [7-8]. Additionally, we have also developed a cryogenic rotary joint to provide coolant for evaporator [9-10].

The heat transfer capacity of TS cooling system is determined with the minimum value of the heat transfer capacity of condenser, adiabatic tube and evaporator. The heat transfer capacity of the condenser depends on its size and the cooling power of the cryocooler connected to it. In the adiabatic tube, the limit of heat transfer is determined by the counter-flow related to the aspect ratio of adiabatic tube. The heat transfer capacity of the evaporator is also related to the design of the evaporator and the liquid neon quantity. However, the liquid neon quantity depends on the saturation pressure. We consider that the saturation pressure is related to the condensation area with the condenser. Therefore, in the present paper, we studied the saturation pressure and heat transfer capacity with different condensation areas of condenser of TS cooling system. We measured heat transfer capacity defined as heat load value in which we visibly observe the state of boundary between film-boiling and nucleate boiling state.

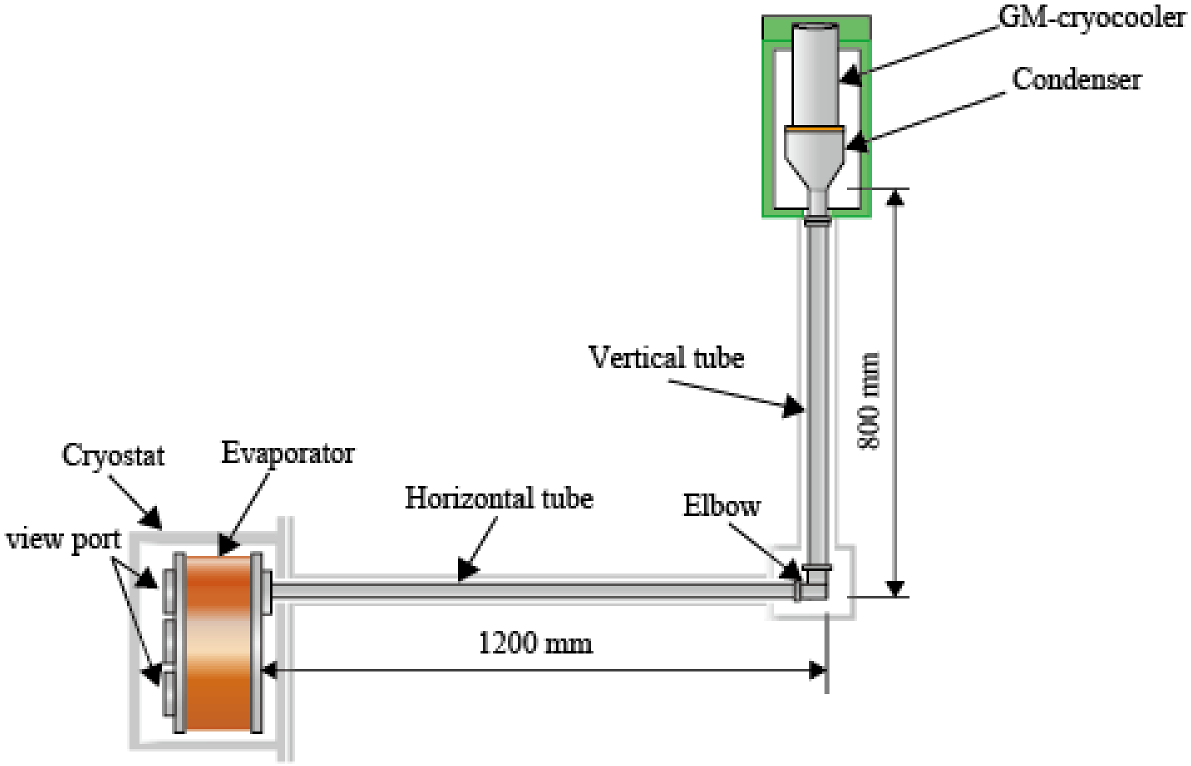

Figure 1. A schematic view of the TS cooling system. This system is composed of two condensers each connected to GM cryocooler, adiabatic tubes aligned vertical and horizontal and an evaporator. All of TS parts are under vacuum. The evaporator has 2 view ports to directly observe a liquid-gas mixing neon in the evaporator.

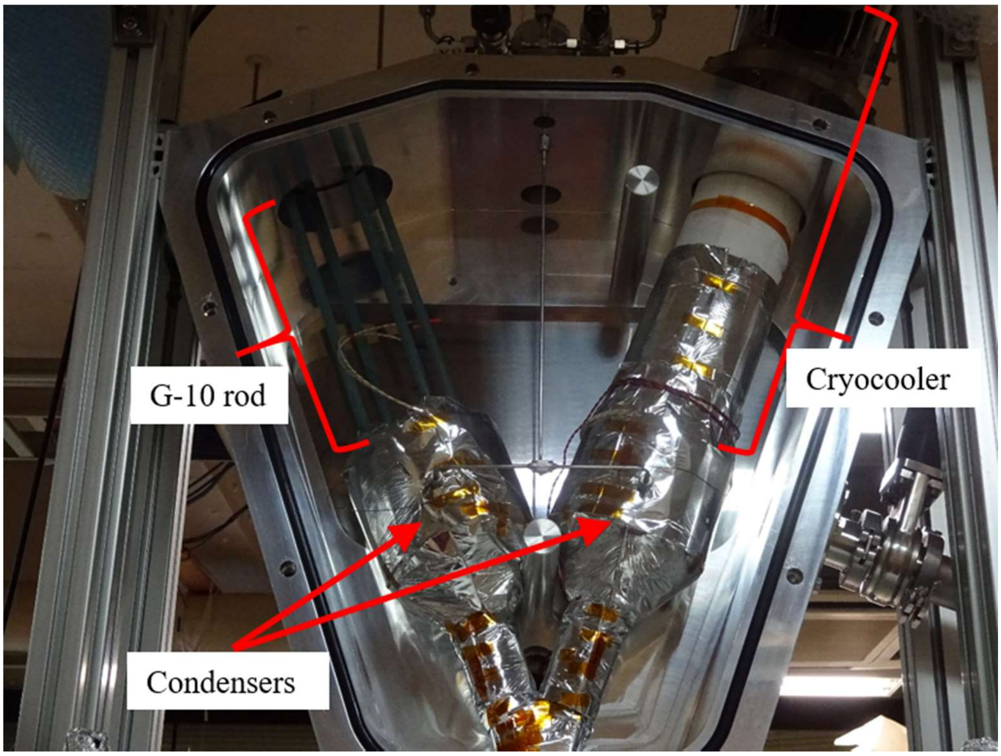

Figure 2. A part of neon condensation unit of thermosypon cooling system. There are two condensers indicated by arrows. To change the condensation area, we change the number of cryocoolers. For the heat load test with single condenser, the cryocooler was removed from condenser and set the G-10 rod instead of cryocooler as shown in the present figure (left).

2. Experiment

2.1. Experimental Set-up

A closed loop TS is composed by condenser, evaporator and adiabatic tubes. The TS cooling system in studied in this paper is shown in figure 1. Each of the two condensers can be connected to corresponding GM-type cryocooler (RDK-500B, SHI). We have arranged two cryocoolers for the present study. The condensers have an optimal fin array to promote the heat exchange [11]. The integrated condensation area of each condenser is 88000 mm^2. A silicon diode sensor (DT-670-CU, Lakeshore) was embedded in the heat exchange copper plate between the cold head and the condenser to measure the condenser temperature. The temperature of the condenser was controlled by using a cartridge heater with temperature controller (Model 331S, Lakeshore).

The adiabatic tube is divided into a vertical and a horizontal section, both being connected by an elbow tube. The horizontal tube is 25.4 mm in diameter and 1200 mm in length. The vertical tube is 34 mm diameter and 800 mm in length. The evaporator is connected to the end of the horizontal tube. This evaporator is composed of cylindrical part made from oxygen free high conductivity copper sandwiched between two flanges made of stainless steel. The inner diameter and length of evaporator are 400 mm and 150 mm, respectively. Two holes are opened and covered by the Pyrex® glass to visually observe a state of liquid neon as shown in figure 1. To apply a heat load, two cartridge heaters are attached at the bottom surface of the evaporator. Three temperature sensors (Cernox ™ CX-1050-SD, Lake Shore) are embedded around the evaporator to measure the temperature distribution. We measured the saturation pressure of both the evaporator and condenser, using digital pressure gage (GC72, Nagano Keiki). In this paper, we measured heat transfer capacity defined as heat load value in which we observe the state of boundary between film-boiling and nucleate boiling state. We performed these measurements with single condenser as shown in figure 2 and double condensers with two GM cryocoolers. For single condenser experiment, we set the G-10 rod for one condenser instead of cryocooler as shown in figure 2.

2.2. Experiment Procedure
It is necessary to cool down from room temperature to operating temperature before the heat load test. In the cooling procedure, we supplied 434 NL (NL= Normal Litre: 1 litre at 1 atm and 0 ºC) of neon gas, counted by a mass flow meter (SEC-E40, Horiba STEC) at 0.207 MPa.

We conducted the heat load tests with different amounts of neon 435, 440, 451, 470 and 496 NL. The condenser temperature was regulated at 29.6 K during these heat load experiments. We applied by using the cartridge heaters attached at the bottom of the evaporator. Heat loads were systematically increased in 10 W increments. Heat load tests with neon of 470 NL were conducted at two condenser operating temperatures, 29.8 K and 30.0 K.

3. Results and Discussion

3.1. Cooling
The TS cooling system was cooled down from room temperature to operating temperature prior heat load experiments. The temperature evolution of the condenser(s) and the evaporator is shown in figure 3 wherein curves for single condenser and double condenser configurations are plotted as a function of time. It took 45 hours for the evaporator to reach the lowest stationary temperature by using single condenser. With the double condenser, it took 19.5 hours. The cooling power of double condenser with two GM cryocoolers are183 W and 95 W for single condenser with single GM cryocooler.

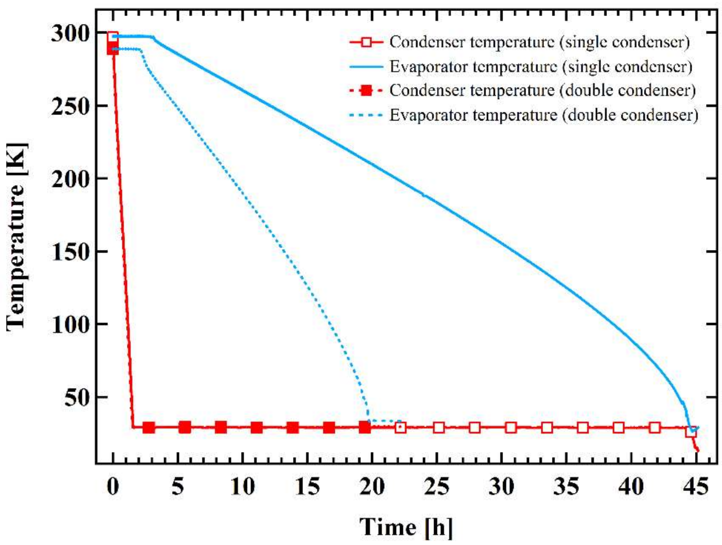

Figure 3. Temperature evolution from room temperature to TS operation temperatures 29.6 K at the condenser and 30.8 K at the evaporator.

3.2. Heat load test
We conducted heat load tests with 5 different neon quantities. Heat load was applied to evaporator in 10 W increments until the boiling changed from nucleate boiling to film boiling. The heat transfer capacity is defined as heat load value in which we visibly observe the state of boundary between film-boiling and nucleate boiling state. The heat transfer capacity at each neon quantity is shown in figure 4. It is evident from this result that at the same supplied neon quantity, reducing the number condensers from two to one causes a decrease in the heat transfer capacity. The liquid neon quantity in the evaporator and the saturation pressure at 451 NL are shown figure 5. From this result, the saturation pressure, which is saturation pressure of single condenser cooling is higher than that of double condenser cooling at the

same heat load. It is worth to note that in the two cooling procedures, the liquid neon quantity has almost the same value for the same saturation pressure value. We found that there is a strong correlation between saturation pressure and the liquid neon quantity in the evaporator. In summary, a reduction in condensation area is accompanied by an increase in saturation pressure and a decrease in evaporator liquid neon quantity. Moreover, the heat transfer capacity depends on the liquid neon quantity in the evaporator. It should, however, be noted that although the condenser number was halved, the heat transfer capacity didn't simply become half. This is coming from that the decrease of condensation area induces increase of both saturation temperature and pressure under the stationary heat load.

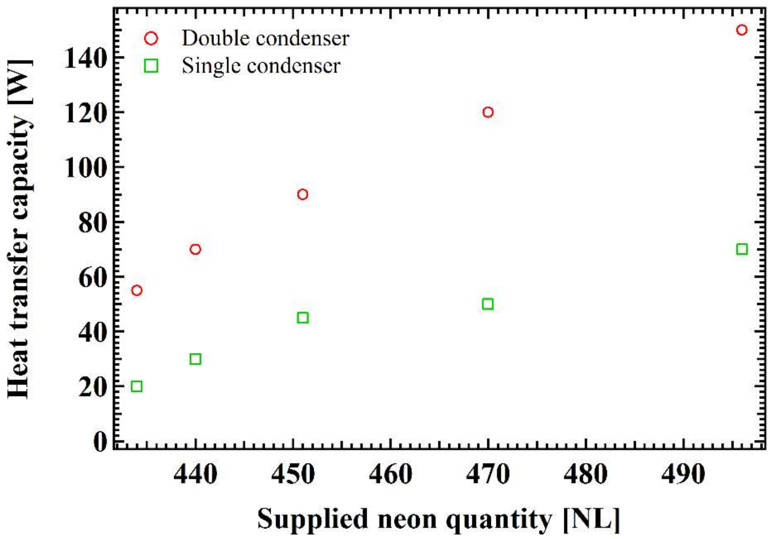

Figure 4. Heat transfer capacity as a function of neon quantity with single and double condensers.

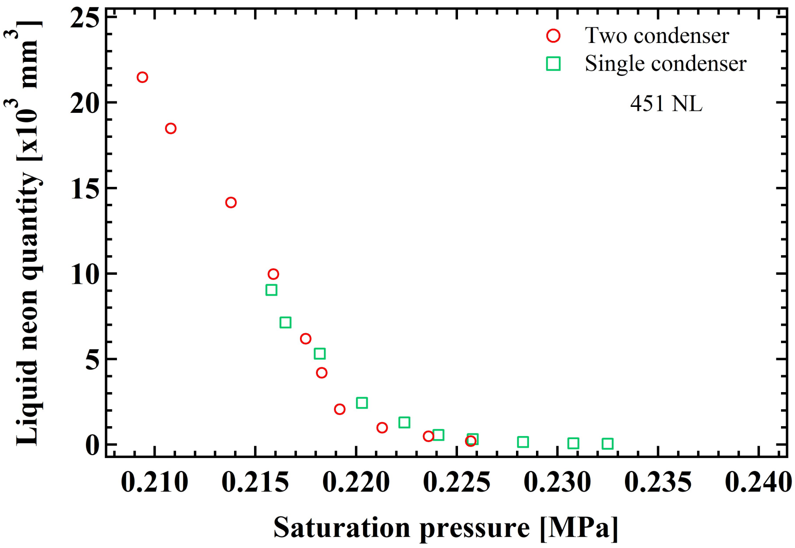

Figure 5. Liquid neon quantity and corresponding saturation pressure when the neon quantity is 451 NL.

3.3. The operating temperature

We also carried out the heat load tests at three different condenser operating temperatures for 470 NL neon. In this heat load test, by using double condensers, the condenser operating temperature was changed to 29.8 K and 30.0 K in addition to 29.6 K as shown in the previous sections. The heat transfer capacity with 29.8 K and 30.0 K was also changed to 40 W and 20 W, respectively. Figure 6 shows the relationship between the saturation pressure and liquid neon quantity in the evaporator with different condenser temperatures with 470 NL neon. With increasing the saturation pressure, liquid neon quantity decreases. From these results, the condenser temperature may affect the saturation pressure and liquid neon quantity.

The saturation pressure with different condenser temperatures as a function of temperature difference between saturation temperature and condenser temperature is shown in figure 7. The saturation pressure is in proportion to the temperature difference. Even the condenser temperature is different, the temperature difference is the same if the applied heat load is the same following the heat transfer equation $Q = h A (T_{sat} - T_{cond})$, where Q, h and A are constant as heat load associated with heat invasion, thermal transfer coefficient and condensation area, T_{sat} and T_{cond} are saturation temperature of refrigerant and condenser temperature. Even the no heat load for evaporator, the temperature difference shows the about 0.26 K. This initial temperature difference indicates the heat invasion. Comparing the saturation pressures with different condensation temperatures with 0 W, the saturation pressure was increased as condenser temperature increased. This increment is corresponding to the saturation temperature.

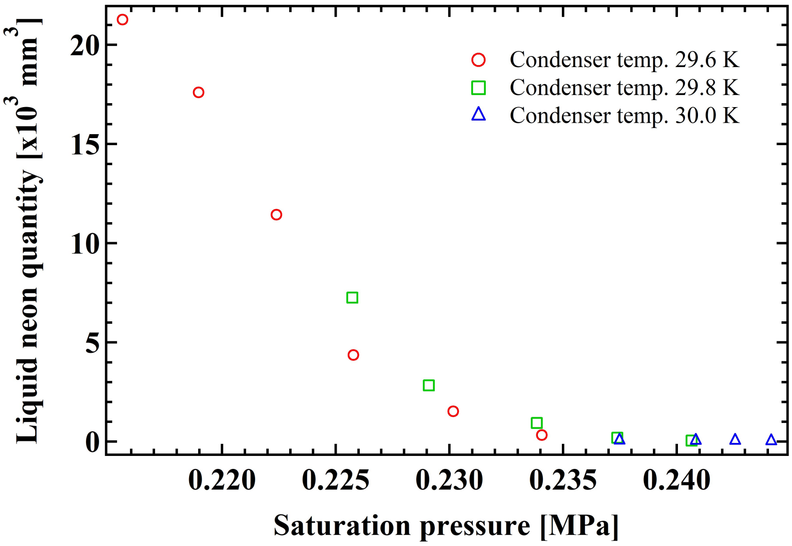

Figure 6. The relationship between the saturation pressure and liquid neon quantity in the evaporator with different condenser temperatures with 470 NL neon.

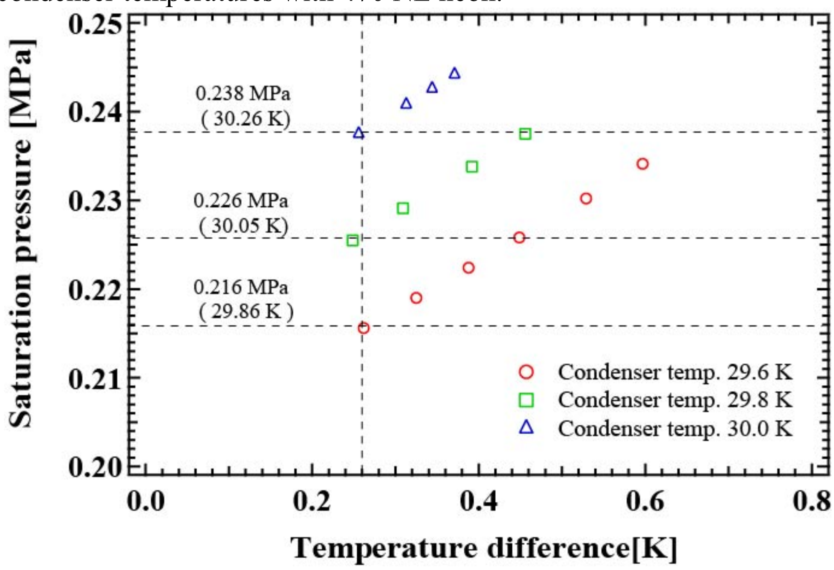

Figure 7. The relationship between the saturation pressure and the temperature difference between saturation temperature and condenser temperature with 470 NL neon.

3.4. The relationship between the saturation pressure and the temperature difference

The saturation pressure as a function of temperature difference for single and double condenser cooling is shown in figure 8. The relationship between the saturation pressure and the heat load with single and double condenser cooling is shown in figure 9. The temperature difference of single condenser results become twice from the double condenser results. This mean if the applying heat load is the same, the temperature difference depends on the heat transfer area as shown in a heat transfer formula in *3.3*. Reducing the heat transfer area in half, which we reduce the condenser from double to single, the temperature difference became twice. Thanks to figure 9, we are able to predict the saturation pressure once we get a heat load value from the HTS machine cooling system design. This immediately leads to estimation of liquid neon quantity.

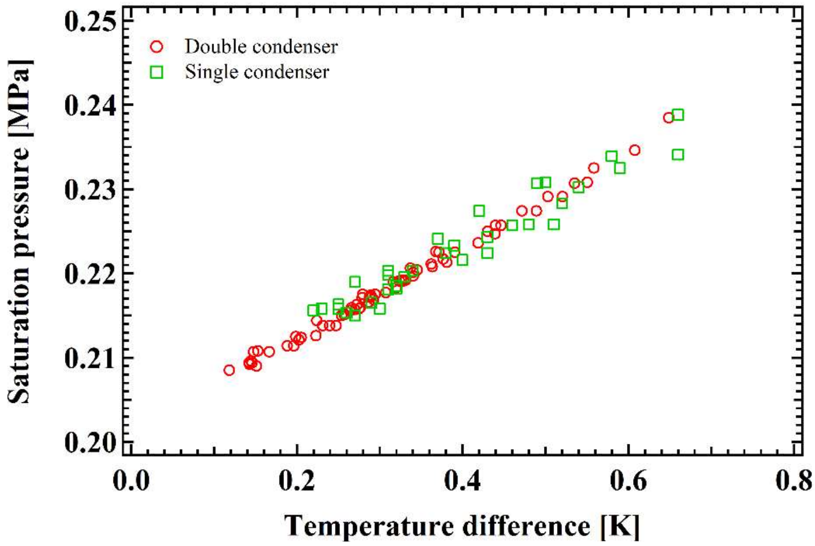

Figure 8. The relationship between the saturation pressure and the temperature difference for single and double condenser cooling.

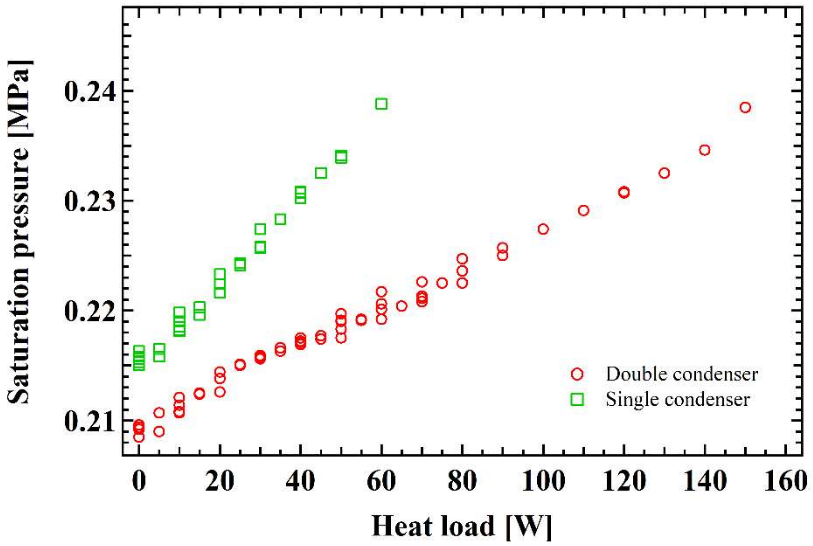

Figure 9. The relationship between the saturation pressure and heat load

4. Conclusion

To obtain the optimized TS cooling system of HTS electric machines, a heat transfer capacity has to be studied for individual components. We studied the relationship between saturation pressure and heat transfer capacity of TS cooling system with a different condensation area. The heat load test was conducted with five different quantities of neon in the TS cooling system. We have changed the condensation area by using two cryocoolers. According to a 2-fold change of condensation area, the saturation pressure was varied under the change of temperature difference between the saturation temperature and condenser temperature. This leads to change both liquid neon quantity and heat transfer capacity. Thus, if we design a large condensation area, we obtain high heat transfer capacity. From the heat load test with three different operating temperatures, we also obtained that the temperature difference between the saturation temperature and condenser temperature is constant under the same heat load and same condensation area. This means the low operating temperature makes high heat transfer capacity. From these results, we estimate the saturation pressure and liquid neon quantity from the design of condensation area and the heat load of HTS machine.

References

[1] Gamble B, Snitcher G and MacDonald T, “Full power test of a 36.5 MW HTS propulsion motor,” *IEEE Trans. Appl. Supercond.*, vol. **21**, no. 3, pp. 1083–88, Jun. 2011.

[2] Nick D, Grundmann J, Fraunhofer J, “Test results from Siemens low-speed, high-torque HTS machine and description of further steps towards commercialization of HTS machines,” *Physica C*, vol. **482**, pp. 105-10, May 2012.

[3] Umemoto K, Aizawa K, Yokoyama M, Yoshikawa M, kimura Y, Izumi M, Ohasi K, Numano M, Okumura K, Yamaguchi M, Gocho Y and Kosuge E, “Development of 1MW-class HTS motor for podded ship propulsion system,” *J. Phys. Conf. Ser.*, vol. **234**, 032060, 2010.

[4] Yanamoto T, Izumi M, Yokoyama M and Umemoto K, "Electric Propulsion Motor Development for Commercial Ships in Japan,"*Proceedings of the IEEE*, vol.**103**, pp.2333-43, 2015

[5] Felder B, Miki M, Deng Z, Tsuzuki K, Shinohara N, Izumi M, and Hayakawa H, “Development of a cryogenic helium-neon gas mixture cooling system for use in a Gd-Bulk HTS synchronous motor”, *IEEE Trans. Appl. Supercond.,* vol.**21**, no. 3, pp. 2213-16, Jun. 2011.

[6] Sato R, Felder B, Miki M, Tsuzuki K, Hayakawa H, and Izumi M, “Helium-neon gas mixture thermosyphon cooling and stability forLarge scale HTS synchronous motors”, *IEEE Trans. Appl. Supercond.,* vol. **23**, no. 3, 5200704, 2013.

[7] Yamaguchi K, Sato R, Miki M, Yamagata K, Ikeda T, Izumi M, Murase Y, Umemoto K, Yokoyama M, ”Study of the thermosyphon cooling system with a vessel in the sea states,” *Physics Procedia*, vol. **67**, pp. 245-49, 2015.

[8] Yamaguchi K, Miki M, Yamagata K, Ikeda T, Kashima H, Izumi M, Murase Y, Yanase E and Yanamoto T, “Study of HTS machine system cooling with a closed loop thermosyphon: Stability of unsteady heat load and transient conduction”, *IEEE Trans. Appl. Supercond.,* vol. **26**, no. 3, 5204405, 2016.

[9] Miki M, Felder B, Tsuzuki K, Izumi M and Hayakawa H, “Development of the cryo-rotary joint for a HTS synchronous motor with Gd-bulk HTS field-pole magnets,” *J. Phy, Conf. Ser.*, vol. **234**, 2010.

[10] Cryo-rotary joint, by Izumi M, Miki M, Kitano M (2013,Dec. 31). Patent US 8616587B2.

[11] Felder B, Miki M, Tsuzuki K, Izumi M, and Hayakawa H, “Optimization of a condensed–neon cooling system for a HTS synchronous motor with Gd-bulk HTS field magnets,” *J. Phys. Conf. Ser.*, vol. **234**, 032009, 2010